Strong atmospheric chemistry feedback to climate warming from Arctic methane emissions

Ivar S. A. Isaksen,[1,2] Michael Gauss,[1,3] Gunnar Myhre,[1,2] Katey M. Walter Anthony,[4] and Carolyn Ruppel[5]

[1]   The magnitude and feedbacks of future methane release from the Arctic region are unknown. Despite limited documentation of potential future releases associated with thawing permafrost and degassing methane hydrates, the large potential for future methane releases calls for improved understanding of the interaction of a changing climate with processes in the Arctic and chemical feedbacks in the atmosphere. Here we apply a "state of the art" atmospheric chemistry transport model to show that large emissions of CH_4 would likely have an unexpectedly large impact on the chemical composition of the atmosphere and on radiative forcing (RF). The indirect contribution to RF of additional methane emission is particularly important. It is shown that if global methane emissions were to increase by factors of 2.5 and 5.2 above current emissions, the indirect contributions to RF would be about 250% and 400%, respectively, of the RF that can be attributed to directly emitted methane alone. Assuming several hypothetical scenarios of CH_4 release associated with permafrost thaw, shallow marine hydrate degassing, and submarine landslides, we find a strong positive feedback on RF through atmospheric chemistry. In particular, the impact of CH_4 is enhanced through increase of its lifetime, and of atmospheric abundances of ozone, stratospheric water vapor, and CO_2 as a result of atmospheric chemical processes. Despite uncertainties in emission scenarios, our results provide a better understanding of the feedbacks in the atmospheric chemistry that would amplify climate warming.

Citation: Isaksen, I. S. A., M. Gauss, G. Myhre, K. M. Walter Anthony, and C. Ruppel (2011), Strong atmospheric chemistry feedback to climate warming from Arctic methane emissions, *Global Biogeochem. Cycles*, *25*, GB2002, doi:10.1029/2010GB003845.

1.   Introduction

[2]   Methane (CH_4) is an important greenhouse gas with a radiative forcing (RF) of 0.48 Wm^{-2}, due to anthropogenic activity since preindustrial time [*Forster et al.*, 2007], being second only to CO_2 among the anthropogenic greenhouse gases. Its distribution and growth are well documented [*Forster et al.*, 2007; *Ramaswamy et al.*, 2001] showing a significant increase in atmospheric concentrations since preindustrial times. Analyses of ice core data for the last 650,000 years show that atmospheric CH_4 concentrations varied from approximately 400 ppb during glacial periods to approximately 700 ppb during interglacial periods. The tro-pospheric average concentration is currently about 1,800 ppb, representing an approximate 2.5 increase since preindustrial time. The atmospheric concentrations in 2005 correspond to an atmospheric burden of 4,900 Tg CH_4 (1 Tg = 10^{12} g). Observations since 1984, for which there are continuous measurements, show an increase in atmospheric abundances of CH_4 by about 10%. Growth rates have decreased significantly since the early 1990s, but with pronounced interannual variations [*Rigby et al.*, 2008].

[3] CH_4 is a chemically active greenhouse gas, and its long-term distribution is affected by changes in both emissions and the atmospheric oxidation rate. Estimates of current global CH_4 emissions are in the range 500 to 600 Tg CH_4 yr^{-1} [*Denman et al.*, 2007].

[4]   Atmospheric CH_4 is removed through oxidation by the hydroxyl radical (OH), mainly in the troposphere:

(R1) $CH_4 + OH \rightarrow H_2O + CH_3$

[5]   A small fraction is also removed by surface deposition. In the stratosphere, where water vapor is in the range of only a few ppm, CH_4 oxidation contributes to water vapor buildup. Since reaction (R1) also represents a significant

---

[1]Department of Geosciences, University of Oslo, Oslo, Norway.
[2]Center for International Climate and Environmental Research–Oslo, Oslo, Norway.
[3]Norwegian Meteorological Institute, Oslo, Norway.
[4]Water and Environmental Research Center, Institute of Northern Engineering and International Arctic Research, University of Alaska, Fairbanks, Alaska, USA.
[5]U.S. Geological Survey, Woods Hole, Massachusetts, USA.

loss path for OH, additional CH_4 emission will suppress OH and thereby increase the CH_4 lifetime, implying further increases in atmospheric CH_4 concentrations [*Isaksen and Hov*, 1987; *Prather et al.*, 2001]. This represents a positive chemical feedback, with a feedback factor estimated to be about 1.4 (uncertainty range 1.3 to 1.7) for current atmospheric conditions [*Prather et al.*, 2001]. The nonlinearity in the chemical system could result in a significantly enhanced feedback factor for large CH_4 emissions causing large perturbations [*Isaksen*, 1988].

[6] The growth in atmospheric CH_4 concentrations, a result of an imbalance between sources and sinks, observed over several decades, is reduced markedly during recent years [*Dlugokencky et al.*, 2003]. For instance, estimates reported in IPCC AR4 give close to a balance (about 1 Tg CH_4 yr^{-1} difference between emissions and loss) for the time period 2000 to 2005 [*Denman et al.*, 2007], compared to 33 Tg CH_4 yr^{-1} during the 1980s. Although there are no clear indications whether the changes in trends are due to stabilization in emissions or enhanced atmospheric loss through increased OH levels [*Prather et al.*, 2001], *Dlugokencky et al.* [2003] point to a possible stabilization of emissions in recent decades. This could be a result of changes in emissions from anthropogenic sources and from wetlands [*Bousquet et al.*, 2006]. However, analyses of atmospheric CH_4 changes in 2007 indicate a renewed growth of CH_4 [*Rigby et al.*, 2008].

[7] Increased CH_4 emissions affect climate in several ways: Directly through increased CH_4 concentrations and indirectly through the chemical feedback on CH_4 levels and through production of O_3 and stratospheric H_2O. Furthermore, CO_2 will increase since it is the end product of atmospheric CH_4 oxidation. In the current atmosphere the indirect RF is approximately the same as the direct methane RF, taking into account the effect on its own lifetime, on ozone, and on stratospheric water vapor [*Forster et al.*, 2007].

[8] In this study we use a global Chemical Transport Model (CTM), the Oslo CTM2 [*Isaksen et al.*, 2005; *Søvde et al.*, 2008], to estimate the impact of additional CH_4 emissions on the atmospheric concentrations of the climate gases CH_4, O_3, stratospheric H_2O, and CO_2, and on RF from these forcing agents. The study covers a wide range of hypothetical methane emission scenarios, up to about 5 times the current emission rate. Although there is no evidence supporting the higher emission in this range, we include them in order to demonstrate the particularly strong positive feedback in the chemical system from large methane releases and the general impact on atmospheric composition and on climate forcing.

[9] We further consider two potentially important natural sources of atmospheric CH_4 in relation to the adopted scenarios: (1) Conversion of organic carbon to CH_4, and release when permafrost thaws; and (2) release of CH_4 hydrates in marine sediments. Earlier studies have demonstrated that large releases of CH_4 from natural sources during warming events can have significant impacts on atmospheric CH_4 levels and may have potential synergistic effects leading to increased and/or sustained global warming. Observed surface temperatures in recent years show significant warming, indicating Arctic warming of more than a factor 2 greater than the global mean value [*Hansen et al.*, 2007]. Permafrost thawing could be more extensive than previously

predicted [*Camill*, 2005; *Osterkamp*, 2005], with large potential for methane emission.

[10] Atmospheric CH_4 has a global average atmospheric lifetime of approximately 8 to 10 years [*Denman et al.*, 2007]. Thus, atmospheric composition changes initiated by methane emissions from Arctic warming depend critically on the time horizon of the CH_4 releases from thawing permafrost and degassing from marine hydrates (centennial to millennium timescales).

[11] Our calculations are based on a range of hypothetical future emission scenarios for CH_4. There are currently no studies that quantify large CH_4 emission from permafrost thawing and destabilization of marine gas hydrates in the Arctic in a future warmer climate.

2. CH_4 Emissions From the Arctic Region

[12] We consider two major sources of CH_4 emissions from the warming Arctic: (1) Methane produced from microbial degradation of labile organic carbon that becomes bioavailable as permafrost thaws; and (2) methane released from gas hydrate deposits as they dissociate in response to climate warming. Thawing permafrost may also promote emissions from other methane sources in the Arctic, but the amount of methane that could potentially be produced by microbial processes in thawed soils or release of methane from gas hydrates far exceeds that associated with other Arctic sources. There is evidence that continuous permafrost is actively thawing in many circum-Arctic regions, both onshore and in the shallow offshore continental shelves [*Rachold et al.*, 2007].

2.1. Methane and Thawing Permafrost

[13] Thawing of permafrost at a rate of 0.04–0.10 m yr^{-1} has been observed in some terrestrial upland regions [*Osterkamp*, 2005], and it is shown that temperatures have increased at depths as great as 25 to 30 m below the surface at some locations in the Arctic during the last two decades [*Isaksen et al.*, 2007; *Osterkamp and Jorgenson*, 2006]. *Camill* [2005] finds that if the current rate of temperature increase (which is at least twice that of the global mean temperature increase) continues at his sites in boreal peatlands in Arctic Canada, the permafrost will have disappeared by the end of this century. The observations at this measurement site are consistent with a warming of at least 7–8°C in a high-CO_2-emission scenario.

[14] Northern soils sequester an estimated 1,672 Pg (1 Pg = 1e+15 g) of organic C, 88% of which is stored in perennially frozen ground [*Tarnocai et al.*, 2009]. The yedoma ice complex within the continuous permafrost in Northern Siberia is of particular interest for understanding the interplay among thawing permafrost, organic carbon, and methane emissions. The yedoma complex consists of ice-rich frozen loess and loess-related sediments that cover approximately 1 million km^2. These sediments have organic carbon content of approximately 27 kg C/m^3 [*Walter et al.*, 2006] and represent a large reservoir (~450 Pg C) of labile organic carbon [*Zimov et al.*, 1997]. An additional 240 Pg C are sequestered in continuous permafrost in thick fluvial deltaic deposits. Thawing of this permafrost and particularly of the yedoma ice complex could produce large CH_4 emissions via anaerobic degradation of the labile carbon, as

demonstrated in laboratory incubations by *Zimov et al.* [1997]. In order to have sustained anaerobic conditions in thermokarsting soils, meltwater needs to be retained in the yedoma complex.

[15] Thermokarst lakes (lakes that have an underlying thaw bulb and that are widespread in some parts of the Arctic) are among the best places to study the potential release of CH_4 during permafrost degradation. *Plug and West* [2009] consider thermokarst expansion rates of up to 8 m in a single year. A strong amplification of CH_4 emissions from Arctic lakes due to thawing of permafrost has already been observed in response to ongoing climate warming. For instance, *Walter et al.* [2006] described significant increases (~60%) in CH_4 emissions from North Siberian thermokarst lakes between 1974 and 2000, associated with a more moderate (15%) increase in lake area during the same period. Calculations by *Walter et al.* [2007] suggest that ~50 Pg CH_4 will be released from Siberian thermokarst (thaw) lakes as yedoma permafrost thaws over a timescale of centuries to millennia. CH_4 emission from lakes in other nonyedoma permafrost-dominated regions in the Arctic is also expected as thermokarst lakes form and expand in conjunction with warming and thawing of permafrost.

[16] The remainder of nonyedoma permafrost in the Arctic contains ~1,000 Pg C [*Tarnocai et al.*, 2009]. Assuming that 10% of this permafrost will thaw beneath lakes and 17% of the C in the thawed permafrost will be converted to CH_4, similar to the efficiency of CH_4 production in yedoma, we estimate that 23 Pg CH_4 can be released from nonyedoma thermokarst lakes. Together, thawing of yedoma and nonyedoma permafrost could thus release up to 73 Pg CH_4 to the atmosphere.

[17] Several studies indicate that high-latitude wetlands have CH_4 emissions that are sensitive to increased temperatures. For example, northern peatlands that experience permafrost thaw [*Christensen et al.*, 2004; *Wickland et al.*, 2006] have enhanced CH_4 emissions. Due to uncertainties associated with future surface moisture and redox regimes, enhanced wetland emissions are not explicitly included as a methane source here.

[18] The CH_4 emission rate and the magnitude of its accumulation in the atmosphere strongly depend on the rate of permafrost thaw. Under current assumptions of warming in the Arctic, permafrost thaw and CH_4 release are likely to occur over timescales of centuries to millennia. In scenarios of more enhanced warming of the Arctic than considered in current climate models [*IPCC*, 2007] the timescale for CH_4 release due to permafrost thawing could be shorter. Although the current global contribution from North Siberian thermokarst lake emissions of CH_4 are small, *Walter et al.* [2006] indicate that these emissions have increased significantly (~60%) between 1974 and 2000.

2.2. Methane Hydrates

[19] Gas hydrates (clathrates) are a solid, ice like form of mostly methane, which occur beneath and possibly within [*Dallimore and Collett*, 1995] onshore permafrost and also in subsea permafrost that persists in some high-latitude regions to water depths as great as ~90 m. Both permafrost-associated gas hydrates and the shallowest part of the deepwater marine gas hydrate system are susceptible to

dissociation (breakdown to methane and water) under conditions of a warming Arctic climate.

[20] The most recent review of the numerous published estimates of the amount of methane sequestered in global gas hydrate deposits converges on a range of 3 to $40 \times 10^{15} \, m^3$ of methane [*Boswell and Collett*, 2011], which converts to a range of ~1,600 to 21,000 Pg C. This consensus range brackets some older estimates (3000 Pg C in the work of *Buffett and Archer* [2004]) and a recent estimate of 1,000 to 10,000 Pg C by *Krey et al.* [2009]. Based on the estimates by *Soloviev et al.* [1987], *Shakhova et al.* [2010a] conclude that one quarter of the Arctic ocean shelf contains 540 Pg CH_4 in gas hydrates. This yields an estimated ~1,600 Pg C within gas hydrates associated with subsea permafrost on the Arctic Ocean continental shelves. It is important to note that the formerly terrestrial sediments on these very shallow shelves contain significant additional carbon in nonhydrate form. Like the carbon trapped in terrestrial permafrost, this additional carbon is subject to microbial degradation and CO_2 and CH_4 production as the subsea permafrost thaws.

[21] In the deep geologic past, CH_4 releases from gas hydrates may have been triggered by, but also possibly exacerbated, the extreme warming event at ~55 Ma before present [*Dickens et al.*, 1995, 1997; *Lamarque et al.*, 2006; *Renssen et al.*, 2004; *Schmidt and Shindell*, 2003]. In this study we estimate a range of potential future methane emissions from the various Arctic gas hydrate populations:

[22] 1. Subsea Permafrost: There is substantial evidence that subsea permafrost is undergoing rapid degradation at high northern latitudes [e.g., *Rachold et al.*, 2007; *Shakhova et al.*, 2005]. The current rate of subsea permafrost degradation is unknown, and acceleration in this degradation with recent changes in sea ice cover and thus ocean temperatures is expected, but not yet fully documented. Still, dissociation of methane hydrate that is currently capped by or contained within subsea permafrost is very likely occurring now [e.g., *Shakhova et al.*, 2010b] and should increase as warming affects the ocean-atmosphere system. Methane released from these hydrates would be emitted into shallow seas where relatively little is likely to be oxidized before reaching the atmosphere. *Shakhova et al.* [2008] speculate that 50 Pg CH_4 could be released abruptly at any time from gas hydrates associated with subsea permafrost. Although there is no basis for estimating the rate of such a release, this value is used as a worst case scenario for the numerical model studies.

[23] 2. Methane hydrates in terrestrial permafrost near the top of the gas hydrate stability zone are unlikely to contribute significantly to the net methane flux from these deposits. A critical exception may be beneath deep thermokarst thaw bulbs, where the superposition of climate-induced surface warming and possible thaw bulb growth may so perturb temperatures near the top of the gas hydrate stability zone that methane hydrate at depths of only a few hundred meters might be susceptible to dissociation.

[24] 3. Deepwater marine hydrates: Most deepwater gas hydrates are unlikely to be a major source of atmospheric methane in climate scenarios that consider less than several millennia. Dissolution and oxidation are likely to strongly reduce the amount of methane that reaches the atmosphere once it is emitted at the seafloor. One exception is gas hydrate in continental margin sediments at pressure-temperature conditions close to the gas hydrate phase boundary. For

example, contemporary climate warming may be triggering gas hydrate dissociation and methane emissions along the West Spitsbergen margin [*Westbrook et al.*, 2009]. In that case, much of the methane is emitted rapidly and in bubble streams, meaning that significant amounts could reach the atmosphere. In other cases, oxidation and dissolution might be expected to prevent much methane from crossing the ocean-atmosphere interface. The numerical model studies presented here do not include a potential contribution from this population of potentially degrading gas hydrates.

[25] Submarine landslides associated with gas hydrates and/or underlying free gas are possible for CH_4 release from marine sediments (e.g., discussion and references in the work of *Archer* [2007]). It is assumed that single landslides can release up to about 5 Pg C as CH_4, based on estimates of past major landslides. This can be regarded as an upper estimate from single landslides, since a recent estimate indicates lower release [*Paull et al.*, 2007]. Our models do not include this as a potential carbon source.
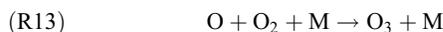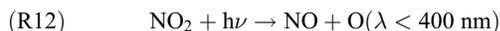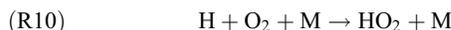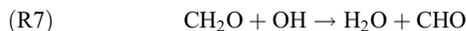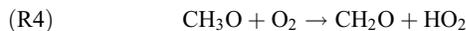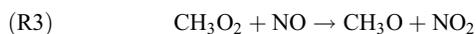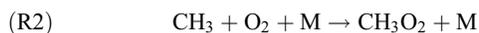
2.3. Model Inputs

[26] Clearly, large uncertainties exist in the amount of carbon stored in Arctic permafrost as methane hydrates, the fraction emitted as CH_4 from thawing permafrost and the timing and magnitude of potential emissions from thawing permafrost and gas hydrates. Combining these with our limited knowledge of the rate and degree of long-term global warming it is clear that our estimates of the impact of future emissions of CH_4 on atmospheric composition and on climate are also associated with large uncertainties. In order to demonstrate the potential contribution of high-latitude release of CH_4 to global warming, several scenarios are considered here. The scenarios discussed in section 5 are based on the potential future emissions of CH_4 estimated for the Arctic permafrost region and for CH_4 stored in hydrates. The estimates include (1) sustained emissions over a specified time horizon from permafrost thawing necessary to reach a defined level of atmospheric CH_4 enhancement and (2) a hypothetical release of 50 Pg of CH_4 from the hydrate pool as a pulse over a limited period of time (1 year) or as sustained emissions over several decades. Although the high-emission scenarios are unlikely to occur, they are compatible with the current knowledge of the cumulative magnitude of CH_4 that might be emitted from permafrost thawing and from CH_4 hydrate destabilization.

3. Atmospheric CH_4 Oxidation

[27] This section provides a brief description of the atmospheric chemistry leading to the formation of greenhouse gases from CH_4 emissions.

[28] CH_4 oxidation leads to enhanced formation of ozone in the troposphere and lower stratosphere through a sequence of reactions involving NO_x compounds. The CH_3 resulting from reaction (R1) is oxidized and the reaction products are photolyzed in the presence of sunlight:

(R2) $CH_3 + O_2 + M \rightarrow CH_3O_2 + M$

(R3) $CH_3O_2 + NO \rightarrow CH_3O + NO_2$

(R4) $CH_3O + O_2 \rightarrow CH_2O + HO_2$

(R5) $CH_2O + h\nu \rightarrow CO + H_2$

(R6) $CH_2O + h\nu \rightarrow CHO + H$

(R7) $CH_2O + OH \rightarrow H_2O + CHO$

(R8) $CHO + O_2 \rightarrow CO + HO_2$

(R9) $CO + OH \rightarrow CO_2 + H$

(R10) $H + O_2 + M \rightarrow HO_2 + M$

(R11) $NO + HO_2 \rightarrow NO_2 + OH$

(R12) $NO_2 + h\nu \rightarrow NO + O(\lambda < 400 \text{ nm})$

(R13) $O + O_2 + M \rightarrow O_3 + M$

[29] M is an air molecule (usually N_2), participating in a three-body reaction, and "$h\nu$" represents the solar photon flux. Through this cycle ozone is efficiently formed in the presence of NO_x, CO and CH_4. The end product of the OH and HO_2 formation from CH_4 is water vapor. As two H_2O molecules are formed from each CH_4 molecule, water vapor enhancements due to additional CH_4 releases can be important in relative terms in the dry stratosphere. Reaction (R9) yields CO_2, constituting another important product from CH_4 oxidation. The result of the CH_4 oxidation chain is thus the formation of the three greenhouse gases O_3, H_2O, and CO_2, which comes in addition to the enhancement of CH_4 concentrations due to direct emissions.

4. Experimental Setup

4.1. Model Description

[30] We apply the global-scale Oslo CTM2 model (Oslo Chemical Transport Model). The model runs with meteorology from the European Centre for Medium Range Weather Forecasts (ECMWF) and uses the Second-Order Moments Scheme [*Prather*, 1986] for advective transport. Surface emissions are based on the EDGARv3.2 database [*Olivier and Berdowski*, 2001] for anthropogenic emissions, and on the work of *Müller* [1992] for natural emissions. CH_4 levels are prescribed in the troposphere with latitudinal distributions based on observations from the ESRL network [*Dlugokencky et al.*, 2010; *Masarie et al.*, 1991]. The model has a resolution, which is 2.8 × 2.8 degrees (T42) horizontally and 60 vertical layers in the troposphere and stratosphere, and has extensive tropospheric and stratospheric chemistry which has been validated in model-model and model-measurement inter comparisons of relevance to CH_4 perturbations [*Gauss et al.*, 2006; *Isaksen et al.*, 2005;

Table 1. Changes in CH_4 Burden Chosen for the $2.5 \times CH_4$, $4 \times CH_4$, $7 \times CH_4$, and $13 \times CH_4$ Cases Addressed by Oslo CTM2 Model Runs, Along With the Lifetimes τ_2 as Modeled by Oslo CTM2 and the Increase With Respect to the Base Case Lifetime τ_1[a]

Name of Case	$\Delta M/M_1$	Lifetime of CH_4 (years), τ_2	τ_2/τ_1 (=β)	Δe in Pg CH_4 yr^{-1}	$\Delta e/e_1$	η
$2.5 \times CH_4$	1.5	12.4	1.36	0.45	0.8	1.8
$4 \times CH_4$	3	14.7	1.61	0.80	1.5	2.0
$7 \times CH_4$	6	18.0	1.98	1.37	2.6	2.4
$13 \times CH_4$	12	22.6	2.50	2.28	4.2	2.9
100 Tg	0.27	9.7	1.07	0.1	0.2	1.5
200 Tg	0.58	10.4	1.15	0.2	0.4	1.6
Hydrate	10.78[b]	21.2[b]	2.34[b]	50 (1 year only)	93	2.7[b]

[a]Also shown are the emission enhancements required to bring about the chosen enhancements in atmospheric CH_4. $M_1 = 4.9$ Pg CH_4, $e_1 = 540$ Tg CH_4 yr^{-1}, and $\tau_1 = 9.1$ years refer to CH_4 burden, emission and lifetime in the base case. ΔM and Δe denote the absolute increases from the base to the perturbation cases. The enhancement factor η (see text) is a measure of the positive feedback in the chemistry of CH_4 and is calculated from the changes in CH_4 lifetime and burden at the new equilibrium. The three last rows show additional cases, which have not been simulated by the Oslo CTM2 model, but are based on emission estimates assuming thawing of permafrost, and a sudden release of CH_4 from marine sediments.
[b]Numbers apply to peak concentrations reached after 1 year.

Shindell et al., 2006]. The model is further documented by *Berglen et al.* [2004] and *Søvde et al.* [2008].

4.2. Simulations and Definitions

[31] In the Oslo CTM2 model simulations atmospheric CH_4 levels are fixed. The estimates of corresponding emissions are made with a forward explicit box model and described in more detail in section 5. Five simulations are made with 2003 meteorology. A base case simulation with present-day CH_4 levels, and 4 perturbation cases with tropospheric CH_4 levels multiplied by 2.5 ("$2.5 \times CH_4$"), four ("$4 \times CH_4$"), seven ("$7 \times CH_4$"), and thirteen ("$13 \times CH_4$"). For chlorine and bromine levels we use values suggested by *WMO* [2003] for 2100, as we are considering long-term future changes. In each of the simulations the global lifetime of CH_4 is calculated from a mass-weighted average of loss through reaction with OH. The base case simulation was spun up for several model years until a stable chemical composition was reached in both the troposphere and the stratosphere. Starting from the resulting chemical fields, both the base case and the perturbation cases were run for an additional 4 years to reach a new equilibrium corresponding to the respective CH_4 levels.

[32] In the calculations we have used current atmospheric water vapor content. Since water vapor is expected to increase in a future warmer climate the calculations were repeated for a 40% increase in tropospheric water vapor (but no other changes). Such perturbations in tropospheric water vapor are expected to be representative for strongly perturbed future climate conditions and key compounds in the interactive climate-chemistry system like OH and O_3 will be affected. We found that the calculated tracer and lifetime perturbations were only slightly affected by this increase (less than 10% impact).

[33] We define an enhancement factor η to quantify the effect of CH_4 emissions on its own concentration and lifetime. η is given as the ratio of relative change in CH_4 burden over relative change in CH_4 emissions, i.e., $\eta = (M_2 - M_1)/M_1/(e_2 - e_1)/e_1$, where M and e represent the global CH_4 burden and global CH_4 emission at steady state, respectively. Subscript 1 is for the base case, and subscript 2 is for the perturbation cases. The feedback in atmospheric concentration from emissions is positive if $\eta > 1$. We define

further the ratio of burden $\alpha = M_2/M_1$ and the ratio of CH_4 lifetimes as $\beta = \tau_2/\tau_1$.

5. Results

5.1. Atmospheric Enhancement of CH_4

[34] Estimates of current atmospheric CH_4 lifetime are in the range 8 to 10 years [*Shindell et al.*, 2006]. In the Oslo CTM2 model the lifetime of CH_4 amounts to 9.1 years in the base case. Table 1 summarizes the main results for the four perturbation cases. For example, in the $4 \times CH_4$ case we choose a fourfold increase in atmospheric CH_4, i.e., $\alpha = 4$ (or $\Delta M/M_1 = 3$) in the Oslo CTM2 model calculation and obtain a new CH_4 lifetime of $\tau_2 = 14.7$ years, giving a relative increase in lifetime of $\beta = 1.61$. The $7 \times CH_4$ case with $\alpha = 7$ almost doubles the CH_4 lifetime, $\beta = 1.98$.

[35] Figure 1 shows β as a function of CH_4 increase. The circles show the increases of CH_4 lifetime as represented by $\beta = \tau_2/\tau_1$ for the four different cases of enhancement modeled by Oslo CTM2. To obtain intermediate values of β we apply cubic interpolation, which is assumed to approximate the relation between β and α ($= M_2/M_1$) well within the considered range.

5.2. Calculated Atmospheric Changes in H_2O, OH, and Ozone

[36] Figure 2 shows model calculated changes in zonal-mean atmospheric water vapor, OH, and ozone for the $4 \times CH_4$, $7 \times CH_4$, and $13 \times CH_4$ cases. Related to the negative height dependence of CH_4 mixing ratio, stratospheric water vapor increases strongly with height. More CH_4 leads to more stratospheric water vapor, and this increase is also significant below 30 km where stratospheric water vapor is radiatively efficient. OH decreases strongly in most of the troposphere due to increased CH_4 oxidation. The strongest decrease in OH is found in the lower troposphere with reductions by more than 50% in the three cases. In the stratosphere, OH increases as a result of enhanced production from water vapor. The ozone increase is particularly large in the upper tropical troposphere where the ozone radiative forcing is strong [*Ramaswamy et al.*, 2001], while in the lower stratosphere the ozone increase is modest, with regions where ozone even decreases slightly when CH_4 is perturbed.
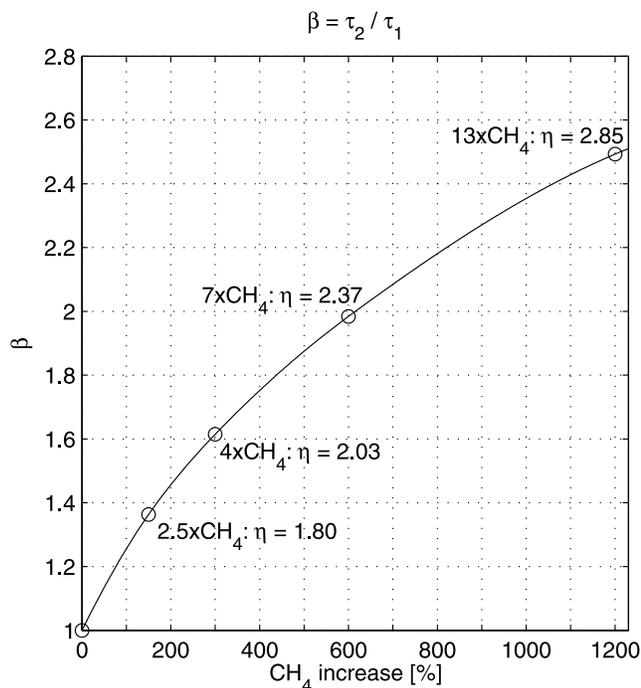
Figure 1. The increase in CH_4 lifetime as a function of the increase in CH_4 burden.

In the upper stratosphere ozone is reduced due to the more efficient removal by HO_x (odd hydrogen) reactions.

5.3. Relating the Chosen CH_4 Enhancements to Emissions and Available Storage

[37] A forward explicit box model is applied to calculate the evolution of CH_4 as function of time assuming different (sustained) CH_4 emission rates. The calculation starts at present CH_4 levels, and at each time step (0.01 years) it uses the CH_4 lifetime that corresponds to the CH_4 concentration calculated by the box model for the current time step. The relation between CH_4 lifetime and concentration calculated in the Oslo CTM2 simulations (Figure 1) is taken as input to the box model. The resulting evolution of CH_4 is shown in Figure 3. 96%, 92% and 87% of the chosen increases are reached after 50 years in the $2.5 \times CH_4$, $4 \times CH_4$ and $7 \times CH_4$ cases, respectively, reflecting the increase in lifetime with increasing emission.

[38] Table 1 also lists the additional CH_4 emissions (Δe) needed to reach the adopted equilibrium enhancement values in the different perturbation experiments. These additional emissions are switched on in the forward explicit box model from the beginning. The base case level is consistent with an emission of 540 Tg CH_4 yr^{-1}. Total equilibrium emissions can thus be obtained by adding 540 Tg CH_4 yr^{-1} to the values given in Table 1. However, an important question in relation to the equilibrium value is the timescale for the additional emission.

[39] Our highest estimate for thermokarst lakes is a 100 to 200 Tg CH_4 yr^{-1} emission, which can be sustained for a
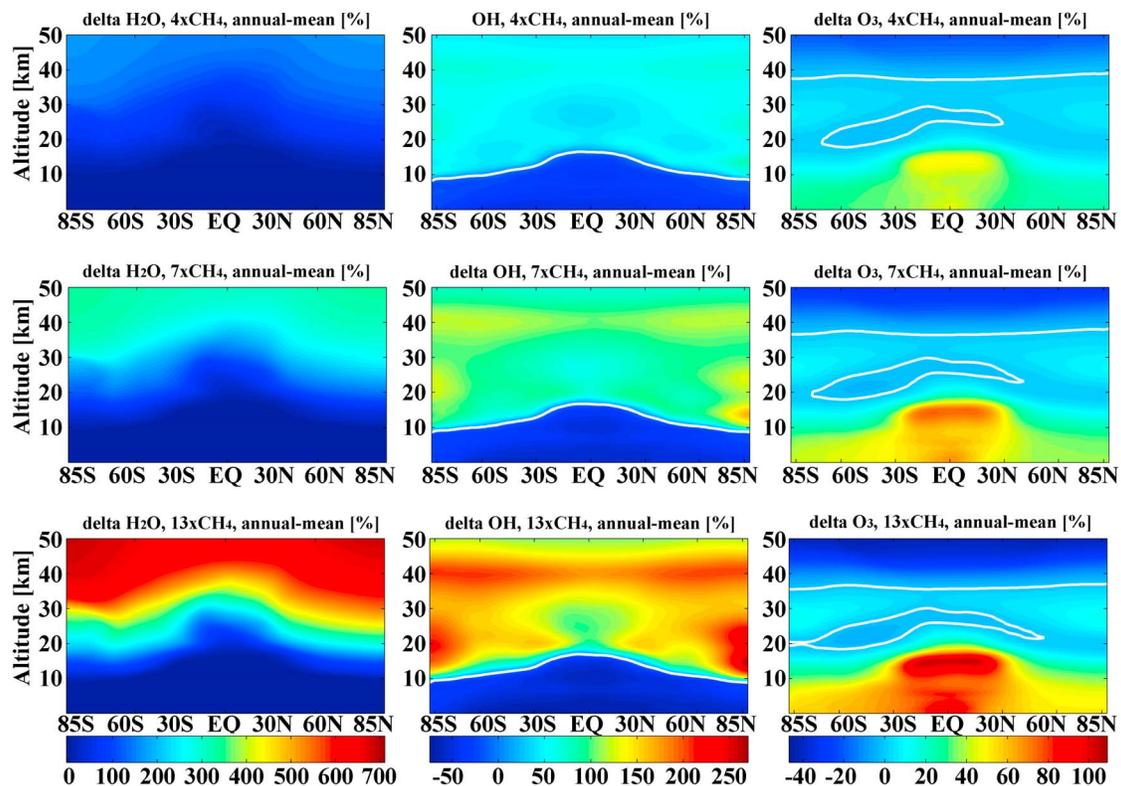
Figure 2. Annual and zonal mean relative change in stratospheric water vapor, the hydroxyl radical, and ozone for 4, 7, and 13 times current CH_4 levels. White contour lines indicate zero change.

Global CH$_4$ burden [multiples of initial burden]
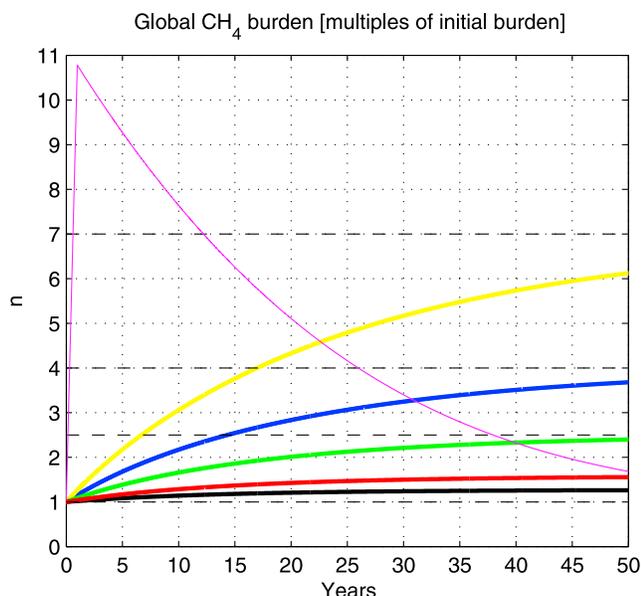
Figure 3. Global CH$_4$ burden as function of time for scenarios 2.5 × CH$_4$ (green), 4 × CH$_4$ (blue), and 7 × CH$_4$ (yellow). Additional scenarios are indicated, for which Oslo CTM2 simulations where not performed, but the lifetime dependence of CH$_4$ on its own concentration is taken into account: 100 Tg(CH$_4$) yr^{-1} sustained (black), 200 Tg (CH$_4$) yr^{-1} sustained (red), and a 1 year 50 Pg(CH$_4$) yr^{-1} emission scenario ("hydrate" scenario, purple). Horizontal gray lines denote current global burden (1) and the three enhanced levels 2.5, 4, and 7.

time period of up to 500 years. Such enhanced emissions would increase the CH$_4$ lifetime by about 7 to 15%, and the CH$_4$ burden by factors of 1.3 to 1.6 (Table 1).

[40] To illustrate the atmospheric impact on CH$_4$ of large pulse type releases, we assume a hypothetical case of 50 Pg CH$_4$ emission, corresponding to CH$_4$ hydrate releases from the Siberian Arctic shelf (as defined in section 2). The atmospheric impact for a pulse emission (over 1 year) and for sustained emissions over several decades, are considered. Our calculations (Figure 3) show that a 1 year pulse emission of 50 Pg CH$_4$ would lead to abundances peaking at about 11 times its current level. Table 1 gives the yearly emissions needed to give equilibrium abundances in the atmosphere 2.5 times, 4 times and 7 times current abundances. A total of 50 Pg CH$_4$ can sustain the additional emissions in the three cases for 111, 62.5, and 36.5 years, respectively, giving enhancements that are approaching the equilibrium values.

[41] For the sustained 100 Tg CH$_4$ yr^{-1}, 200 Tg CH$_4$ yr^{-1} and the 1 year 50 Pg CH$_4$ emission cases, the CH$_4$ lifetime dependence derived from the four explicit Oslo CTM2 simulations (shown in Figure 1) is taken into account in the calculation of CH$_4$ evolution.

5.4. Atmospheric Enhancement of CO$_2$

[42] CH$_4$ is oxidized to CO$_2$ in the atmosphere, and CO$_2$ decays according to different loss processes. Our calculation of the evolution of CO$_2$ (shown in Figure 4) from oxidation of the CH$_4$ released from thawing permafrost or hydrate

storage is based on the formula of IPCC-AR4 [*Forster et al.*, 2007], according to which the decay of a pulse of CO$_2$ with time t is given by

$$a_0 + \sum_{i=1}^{3} a_i \cdot \exp(-t/\tau_i)$$

Where $a_0 = 0.217$, $a_1 = 0.259$, $a_2 = 0.338$, $a_3 = 0.186$, $\tau_1 = 172.9$ years, $\tau_2 = 18.51$ years, and $\tau_3 = 1.186$ years. The pulses at each time step are set equal to the amount that is oxidized from the additional atmospheric CH$_4$ from permafrost emissions. After 50 years, the CO$_2$ values are 4.4, 7.3, and 11.3 ppm (ppm) for the 2.5 × CH$_4$, 4 × CH$_4$, and 7 × CH$_4$ cases, respectively. For comparison with Figure 3, Figure 4 also includes the CH$_4$ hydrate case for which the CO$_2$ enhancement peaks at around 10 ppm after 40 to 50 years. It has to be noted that the CO$_2$ shown in Figure 4 does not include directly emitted CO$_2$ from permafrost thaw. The inclusion of CO$_2$ in these calculations is consistent with the inclusion of CH$_4$ oxidation to CO$_2$ in the GWP for CH$_4$ [*Boucher et al.*, 2009].

5.5. Radiative Forcing

[43] Detailed off-line atmospheric radiative transfer schemes are used in the calculations of radiative forcing (RF), from changes in ozone and stratospheric water vapor (sH$_2$O) [*Myhre et al.*, 2000; *Myhre et al.*, 2007]. For CO$_2$ and CH$_4$, expressions given by *Ramaswamy et al.* [2001] are used. The radiative forcing is not related to a particular year but to the time when the CH$_4$ increase is reached. The 13 ×

Global−mean excess CO$_2$ from CH$_4$ oxidation [ppm]
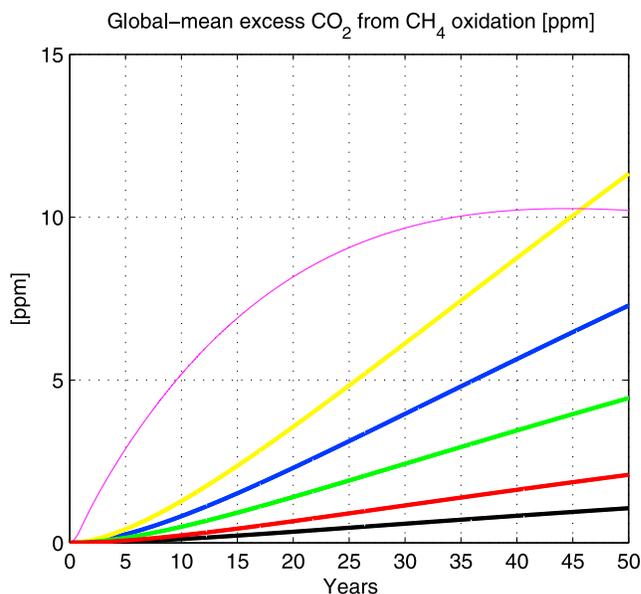
Figure 4. Global-mean mixing ratio of excess CO$_2$ from additional CH$_4$ oxidation for scenarios 2.5 × CH$_4$ (green), 4 × CH$_4$ (blue), and 7 × CH$_4$ (yellow). Additional scenarios are indicated, for which Oslo CTM2 simulations where not performed, but the lifetime dependence of CH$_4$ on its own concentration is taken into account: 100 Tg CH$_4$ yr^{-1} sustained (black), 200 Tg CH$_4$ yr^{-1} sustained (red), and 50 Pg CH$_4$ yr^{-1} switched off after 1 year ("hydrate" scenario, purple).
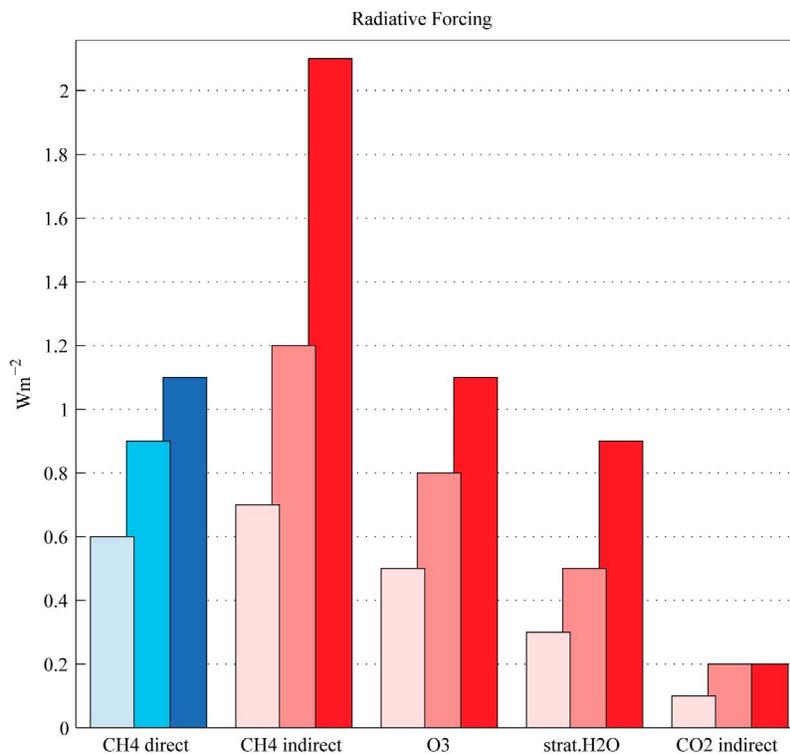
Radiative Forcing

Figure 5. Radiative forcing resulting from CH_4 increases. Blue bars denote contributions from direct emissions, and red bars are contributions from CH_4 initiated changes in atmospheric composition. "CH_4 indirect" represents the CH_4 enhancement that is due to the increase in its lifetime. "CO_2 indirect" relates to the CO_2 enhancement due to oxidation of the additional CH_4. The lightest colors refer to the 4 × CH_4, medium light colors to the 7 × CH_4 and dark colors to the 13 × CH_4 case. The radiative forcing is not related to a particular year but to the time when the CH_4 increase is reached. The 13 × CH_4 case refers to a shorter time horizon (30 years) while the other cases are based on a 50 year time horizon.

CH_4 case refers to a shorter time horizon (30 years) while the other cases are based on a 50 year time horizon.

[44] Results are shown in Figure 5 for the 4 × CH_4, 7 × CH_4 and 13 × CH_4 cases. Radiative forcings due to CH_4 are listed in Table 2. In the 4 × CH_4 case the RF caused by direct emissions of CH_4 and the RF due to the lifetime increase are comparable and add up to 1.3 Wm^{-2}. The RF of 0.5 Wm^{-2} from ozone, calculated for the same case, is probably stronger than the forcing since preindustrial time [*Gauss et al.*, 2006]. For sH_2O we calculate nearly quadrupling (0.3 Wm^{-2}) of the current sH_2O forcing (0.08 Wm^{-2}) [*Myhre et al.*, 2007]. In the 7 × CH_4 and 13 × CH_4 cases the indirect CH_4 RF clearly dominates the direct one, due to more pronounced OH changes. The total RF is 2.2, 3.6, and 5.4 Wm^{-2} for the 4 × CH_4, 7 × CH_4 and 13 × CH_4 cases, respectively.

[45] The importance of CH_4 emissions through atmospheric chemistry perturbation is illustrated by a 3.5- to fivefold increase in the total RF compared to the contribution from direct emissions, increasing in importance with the increase in CH_4 emission. The impact of chemical perturbations by CH_4 emission increases is substantially higher than what is included in the GWP value for CH_4 used in IPCC [*Forster et al.*, 2007], where a twofold increase in RF was adopted to account for indirect effects at current conditions. The CH_4 lifetime feedback represents the most important contribution among the additional radiative for-

cings due to changes in atmospheric composition, followed by ozone (in particular tropospheric ozone) and sH_2O.

[46] According to our simulations, sustained CH_4 emissions of 100 Tg yr^{-1} to 200 Tg yr^{-1} due to permafrost thawing will correspond to a RF of 0.3 to 0.6 Wm^{-2} in a new equilibrium (reached after a few decades). Although the amount of CH_4 released to the atmosphere is large, the short lifetime (8 to 10 years) compared to the time horizon for

Table 2. Radiative Forcing Due to Directly Emitted CH_4 (CH_4 Direct Forcing), the Lifetime Change of CH_4 (CH_4 Indirect Forcing), and the Chemical Enhancements Due to the Feedbacks in the 4 × CH_4, 7 × CH_4, and 13 × CH_4 Cases[a]

Name of Case	CH_4 Direct Forcing	CH_4 Indirect Forcing	Indirect Forcing From O_3, strat. H_2O and CO_2
4 × CH_4	0.6 Wm^{-2}	0.7 Wm^{-2}	0.9 Wm^{-2}
7 × CH_4	0.9 Wm^{-2}	1.2 Wm^{-2}	1.5 Wm^{-2}
13 × CH_4	1.1 Wm^{-2}	2.1 Wm^{-2}	2.2 Wm^{-2}
100 Tg	*0.1 Wm^{-2}*	*0.1 Wm^{-2}*	*0.1 Wm^{-2}*
200 Tg	*0.2 Wm^{-2}*	*0.2 Wm^{-2}*	*0.2 Wm^{-2}*

[a]For the "100 Tg" and "200 Tg" cases (in the table listed in italics) no Oslo CTM2 calculations have been made. Thus the split into direct and indirect components of radiative forcing is based on extrapolated values for β. Contributions to indirect radiative forcing from perturbations of O_3, stratospheric H_2O and CO_2 are not included in the table.

emission (up to 500 years) means that equilibrium in atmospheric concentration is reached at an early stage in the time period. As an illustration of the potential of permafrost CH_4 releases, the increase of the CH_4 concentration by a factor 2.5 compared to current CH_4 concentrations would correspond to an extra emission of 450 Tg CH_4 yr^{-1} from permafrost thawing and give a radiative forcing of about 1.5 Wm^{-2}. However, the emission would be over a shorter time horizon than in the 100 Tg CH_4 yr^{-1} to 200 Tg CH_4 yr^{-1} emission cases.

[47] A release of 50 Pg (CH_4) from gas hydrates over a 30 year time period could give a RF in excess of 4 Wm^{-2}. The larger calculated RF, results from the fact that this case represents a more rapid emission than our 7 × CH_4 case.

[48] The release of up to 5 Pg C estimated for single submarine landslides (see discussion in section 2) can enhance atmospheric CH_4 by nearly 2.5 ppm, and give a RF slightly larger than 1 Wm^{-2}. This is substantially higher than the 0.2 Wm^{-2} (only the direct RF was taken into account) from a similar CH_4 release discussed by *Archer* [2007]. It has to be noted, however, that more recent estimates of the emission from the Storegga Landslide are lower than 5 Pg C [e.g., *Paull et al.*, 2007], and that there is no evidence that the CH_4 released escaped to the atmosphere after the event.

6. Discussion and Conclusion

[49] Relating the magnitude and timing of CH_4 release in a warming Arctic to the adopted scenarios applied in the model studies is challenging due to uncertainties associated with the rate of permafrost warming and thawing, the size and distribution of the large organic C pool [*Tarnocai et al.*, 2009] and its fate in microbial decomposition under aerobic versus anaerobic conditions [*Schuur et al.*, 2008; *Walter et al.*, 2007], and the size and stability of the hydrate reservoir. However, given the magnitude and vulnerability of the permafrost organic carbon pool and the large permafrost-associated CH_4 hydrate reservoir, quantification of the feedbacks associated with the release of CH_4 from these systems is important for climate modeling.

[50] There is a potential for the release of large amounts of carbon stored in the Arctic to the atmosphere as CH_4 following the thawing of permafrost and warming of oceans [*Buffett and Archer*, 2004; *Schuur et al.*, 2008; *Walter et al.*, 2007, 2006]. Considering the positive feedback (increase in lifetime) and the non linearity in atmospheric chemistry through amplification of atmospheric CH_4 (represented by the enhancement factor η), we have applied a wide range of CH_4 emission scenarios to explore the impact of such interactions. The impact on methane lifetime does not only apply to the additionally emitted CH_4 but also to background levels of CH_4.

[51] Although the high-CH_4 scenarios applied in this study are unlikely, they demonstrate the strong CH_4 feedbacks in the climate system, with large amplification of atmospheric composition changes and RF compared to the direct RF of CH_4 emissions.

[52] The Oslo CTM2 has been thoroughly tested with respect to OH and CH_4 lifetime through model comparisons and through perturbation studies [*Hoor et al.*, 2009; *Shindell et al.*, 2006]. These studies show that there are noticeable differences in model estimates. Another model uncertainty

in the Oslo CTM2 calculations may arise from the use of today's meteorology, uncertainties in emissions of other gases than CH_4 (e.g., emissions of NO_x and CO), and the formulation of dry deposition (O_3) and wet deposition (NO_x) [*Isaksen et al.*, 2005; *Solberg et al.*, 2008]. Yet, the uncertainties in the atmospheric chemistry calculations are likely to be small compared to the uncertainties in the amount and time horizon for CH_4 emission from thawing permafrost or degassing hydrates.

[53] Since current atmospheric CH_4 lifetime ranges between 8 and 10 years, the RF of CH_4 emissions from permafrost thawing and CH_4 hydrate degassing depends critically on the rate of emissions. Additional studies linking CH_4 emissions to the possibilities for large future warming in the Arctic are needed.

[54] Although CH_4 emissions from permafrost thawing and hydrate degassing are likely to have a very different spatiotemporal distribution than anthropogenic emissions, the impact on climate will be global in the same way as the impact from CH_4 emitted in other regions, when we take into account the multiyear lifetime of CH_4.

[55] Fossil fuel CO_2 emissions have increased substantially over the last decade and is now 40% higher than in 1990 [*Le Quéré et al.*, 2009; *Myhre et al.*, 2009]. The continued increase in greenhouse gas emissions toward the end of this century has the potential to produce significant warming at high northern latitudes well beyond what has been observed during the last decades [*Hansen et al.*, 2007; *IPCC*, 2007]. There is a possibility that the Arctic temperature increases could be followed by extensive permafrost thawing, with enhanced CH_4 emission from thermokarst lakes [*Walter et al.*, 2006], with later release of CH_4 from gas hydrates that would eventually be affected by warming temperatures. Considering the large, nonlinear atmospheric chemistry feedbacks discussed here, future CH_4 emissions from permafrost deposits could be a larger concern for climate warming than previously thought.

References

Archer, D. (2007), Methane hydrate stability and anthropogenic climate change, *Biogeosciences*, 4(4), 521–544, doi:10.5194/bg-4-521-2007.

Berglen, T. F., T. K. Berntsen, I. S. A. Isaksen, and J. K. Sundet (2004), A global model of the coupled sulfur/oxidant chemistry in the troposphere: The sulfur cycle, *J. Geophys. Res.*, 109, D19310, doi:10.1029/2003JD003948.

Boswell, R., and T. S. Collett (2011), Current perspectives on gas hydrate resources, *Energy Environ. Sci.*, 4, 1206–1215, doi:10.1039/C0EE00203H.

Boucher, O., P. Friedlingstein, B. Collins, and K. P. Shine (2009), The indirect global warming potential and global temperature change potential due to methane oxidation, *Environ. Res. Lett.*, 4, 044007, doi:10.1088/1748-9326/4/4/044007.

Bousquet, P., et al. (2006), Contribution of anthropogenic and natural sources to atmospheric methane variability, *Nature*, 443(7110), 439–443, doi:10.1038/nature05132.

Buffett, B., and D. Archer (2004), Global inventory of methane clathrate: Sensitivity to changes in the deep ocean, *Earth Planet. Sci. Lett.*, 227(3–4), 185–199, doi:10.1016/j.epsl.2004.09.005.

Camill, P. (2005), Permafrost thaw accelerates in boreal peatlands during late-20th century climate warming, *Clim. Change*, 68(1–2), 135–152, doi:10.1007/s10584-005-4785-y.

Christensen, T. R., T. Johansson, H. J. Åkerman, M. Mastepanov, N. Malmer, T. Friborg, P. Crill, and B. H. Svensson (2004), Thawing sub-Arctic permafrost: Effects on vegetation and methane emissions, *Geophys. Res. Lett.*, 31, L04501, doi:10.1029/2003GL018680.

Dallimore, S. R., and T. S. Collett (1995), Intrapermafrost gas hydrates from a deep core hole in the Mackenzie Delta, Northwest Territories, Canada, *Geology*, 23, 527–530, doi:10.1130/0091-7613(1995)023<0527:IGHFAD>2.3.CO;2.

Denman, K. L., et al. (2007), Couplings between changes in the climate system and biogeochemistry, in *Climate Change 2007: The Physical Science Basis. Contribution of Working Group I to the Fourth Assessment Report of the Intergovernmental Panel on Climate Change*, edited by S. Solomon et al., Cambridge Univ. Press, Cambridge, U. K.

Dickens, G. R., J. R. O'Neil, D. C. Rea, and R. M. Owen (1995), Dissociation of oceanic methane hydrate as a cause of the carbon isotope excursion at the end of the Paleocene, *Paleoceanography*, 10, 965–971, doi:10.1029/95PA02087.

Dickens, G. R., M. M. Castillo, and J. C. G. Walker (1997), A blast of gas in the latest Paleocene, *Geology*, 25, 259–262, doi:10.1130/0091-7613 (1997)025<0259:ABOGIT>2.3.CO;2.

Dlugokencky, E. J., S. Houweling, L. Bruhwiler, K. A. Masarie, P. M. Lang, J. B. Miller, and P. P. Tans (2003), Atmospheric methane levels off: Temporary pause or a new steady-state?, *Geophys. Res. Lett.*, 30(19), 1992, doi:10.1029/2003GL018126.

Dlugokencky, E. J., P. M. Lang, and K. A. Masarie (2010), Atmospheric methane dry air mole fractions from the NOAA ESRL Carbon Cycle Cooperative Global Air Sampling Network, 1983–2009, Version: 2010-08-12, ftp://ftp.cmdl.noaa.gov/ccg/ch4/flask/event/, ESRL, NOAA, Boulder, Colo.

Forster, P., et al. (2007), Changes in atmospheric constituents and in radiative forcing, in *Climate Change 2007: The Physical Science Basis. Contribution of Working Group I to the Fourth Assessment Report of the Intergovernmental Panel on Climate Change*, edited by S. Solomon et al., pp. 129–134, Cambridge Univ. Press, Cambridge, U. K.

Gauss, M., et al. (2006), Radiative forcing since preindustrial times due to ozone change in the troposphere and the lower stratosphere, *Atmos. Chem. Phys.*, 6, 575–599, doi:10.5194/acp-6-575-2006.

Hansen, J., et al. (2007), Dangerous human-made interference with climate: A GISS modelE study, *Atmos. Chem. Phys.*, 7(9), 2287–2312, doi:10.5194/acp-7-2287-2007.

Hoor, P., et al. (2009), The impact of traffic emissions on atmospheric ozone and OH: Results from QUANTIFY, *Atmos. Chem. Phys.*, 9(9), 3113–3136, doi:10.5194/acp-9-3113-2009.

IPCC (2007), *The Physical Science Basis. Contribution of Working Group I to the Fourth Assessment Report of the Intergovernmental Panel on Climate Change*, edited by S. Solomon et al., Cambridge Univ. Press, Cambridge, U. K.

Isaksen, I. S. A. (1988), *Is the Oxidizing Capacity of the Atmosphere Changing? Report of the Dahlem Workshop of the Changing Atmosphere, Berlin, Nov. 1–6, 1987*, edited by F. S. Rowland and I. S. A. Isaksen, pp. 141–157, John Wiley, Chichester, U. K.

Isaksen, I. S. A., and Ø. Hov (1987), Calculation of trends in the tropospheric concentration of O₃, OH, CO, CH₄ and NOₓ, *Tellus, Ser. B*, 39, 271–285, doi:10.1111/j.1600-0889.1987.tb00099.x.

Isaksen, I. S. A., C. Zerefos, K. Kourtidis, C. Meleti, S. B. Dalsoren, J. K. Sundet, A. Grini, P. Zanis, and D. Balis (2005), Tropospheric ozone changes at unpolluted and semipolluted regions induced by stratospheric ozone changes, *J. Geophys. Res.*, 110, D02302, doi:10.1029/2004JD004618.

Isaksen, K., J. L. Sollid, P. Holmlund, and C. Harris (2007), Recent warming of mountain permafrost in Svalbard and Scandinavia, *J. Geophys. Res.*, 112, F02S04, doi:10.1029/2006JF000522.

Krey, V., et al. (2009), Gas hydrates: Entrance to a methane age or climate threat?, *Environ. Res. Lett.*, 4(3), doi:10.1088/1748-9326/4/3/034007.

Lamarque, J. F., J. T. Kiehl, C. A. Shields, B. A. Boville, and D. E. Kinnison (2006), Modeling the response to changes in tropospheric methane concentration: Application to the Permian-Triassic boundary, *Paleoceanography*, 21, PA3006, doi:10.1029/2006PA001276.

Le Quéré, C., et al. (2009), Trends in the sources and sinks of carbon dioxide, *Nat. Geosci.*, 2(12), 831–836, doi:10.1038/ngeo689.

Masarie, K. A., et al. (1991), A rule-based expert system for evaluating the quality of long-term, in situ, gas chromatographic measurements of atmospheric methane, *NOAA Tech. Memo. ERL CMDL-3*, NOAA Environ. Res. Lab., Boulder, Colo.

Müller, J. (1992), Geographical distribution and seasonal variation of surface emissions and deposition velocities of atmospheric trace gases, *J. Geophys. Res.*, 97(D4), 3787–3804.

Myhre, G., S. Karlsdottir, I. S. A. Isaksen, and F. Stordal (2000), Radiative forcing due to changes in tropospheric ozone in the period 1980 to 1996, *J. Geophys. Res.*, 105(D23), 28,935–28,942, doi:10.1029/2000JD900187.

Myhre, G., J. S. Nilsen, L. Gulstad, K. P. Shine, B. Rognerud, and I. S. A. Isaksen (2007), Radiative forcing due to stratospheric water vapour from CH₄ oxidation, *Geophys. Res. Lett.*, 34, L01807, doi:10.1029/2006GL027472.

Myhre, G., K. Alterskjaer, and D. Lowe (2009), A fast method for updating global fossil fuel carbon dioxide emissions, *Environ. Res. Lett.*, 4(3), doi:10.1088/1748-9326/4/3/034012.

Olivier, J. G. J., and J. J. M. Berdowski (2001), Global emissions sources and sinks, in *The Climate System*, edited by J. J. M. Berdowski, R. Guicherit, and B. J. Heij, pp. 33–78, A. A. Balkema Publ., Lisse, Netherlands.

Osterkamp, T. E. (2005), The recent warming of permafrost in Alaska, *Global Planet. Change*, 49(3–4), 187–202, doi:10.1016/j.gloplacha.2005.09.001.

Osterkamp, T. E., and J. C. Jorgenson (2006), Warming of permafrost in the Arctic National Wildlife Refuge, Alaska, *Permafrost Periglacial Proc.*, 17(1), 65–69, doi:10.1002/ppp.538.

Paull, C. K., W. Ussler, and W. S. Holbrook (2007), Assessing methane release from the colossal Storegga submarine landslide, *Geophys. Res. Lett.*, 34, L04601, doi:10.1029/2006GL028331.

Plug, L. J., and J. J. West (2009), Thaw lake expansion in a two-dimensional coupled model of heat transfer, thaw subsidence, and mass movement, *J. Geophys. Res.*, 114, F01002, doi:10.1029/2006JF000740.

Prather, M., et al. (2001), Atmospheric chemistry and greenhouse gases, in *Climate Change 2001: The Scientific Basis, Contribution of Working Group I to the Third Assessment Report of the Intergovernmental Panel on Climate Change*, edited by J. T. Houghton et al., pp. 239–287, Cambridge Univ. Press, Cambridge, U. K.

Prather, M. J. (1986), Numerical advection by conservation of 2nd-order moments, *J. Geophys. Res.*, 91(D6), 6671–6681, doi:10.1029/JD091iD06p06671.

Rachold, V., D. Y. Bolshiyanov, M. N. Grigoriev, H.-W. Hubberten, R. Junker, V. V. Kunitsky, F. Merker, P. Overduin, and W. Schneider (2007), Nearshore Arctic subsea permafrost in transition, *Eos Trans. AGU*, 88(13), doi:10.1029/2007EO130001.

Ramaswamy, V., O. Boucher, J. Haigh, D. Hauglustaine, J. Haywood, G. Myhre, T. Nakajima, G. Y. Shi, and S. Solomon (2001), Radiative forcing of climate change, in *Climate Change 2001: The Scientific Basis, Contribution of Working Group I to the Third Assessment Report of the Intergovernmental Panel on Climate Change*, edited by J. T. Houghton et al., pp. 349–416, Cambridge Univ. Press, Cambridge, U. K.

Rennssen, H., C. J. Beets, T. Fichefet, H. Goosse, and D. Kroon (2004), Modeling the climate response to a massive methane release from gas hydrates, *Paleoceanography*, 19, PA2010, doi:10.1029/2003PA000968.

Rigby, M., et al. (2008), Renewed growth of atmospheric methane, *Geophys. Res. Lett.*, 35, L22805, doi:10.1029/2008GL036037.

Schmidt, G. A., and D. T. Shindell (2003), Atmospheric composition, radiative forcing, and climate change as a consequence of a massive methane release from gas hydrates, *Paleoceanography*, 18(1), 1004, doi:10.1029/2002PA000757.

Schuur, E. A. G., et al. (2008), Vulnerability of permafrost carbon to climate change: Implications for the global carbon cycle, *BioScience*, 58(8), 701–714, doi:10.1641/B580807.

Shakhova, N., I. Semiletov, and G. Panteleev. (2005) The distribution of methane on the East Siberian Arctic shelves: Implications for the marine methane cycle, *Geophys. Res. Lett.*, 32, L09601, doi:10.1029/2005GL022751.

Shakhova, N., I. Semiletov, A. Salyuk, and D. Kosmach (2008), Anomalies of methane in the atmosphere over the East Siberian shelf: Is there any sign of methane leakage from shallow shelf hydrates?, *Geophys. Res. Abstr.*, 10, EGU2008-A-01526.

Shakhova, N., I. Semiletov, I. Leifer, A. Salyuk, P. Rekant, and D. Kosmach (2010a), Geochemical and geophysical evidence of methane release over the East Siberian Arctic Shelf, *J. Geophys. Res.*, 115, C08007, doi:10.1029/2009JC005602.

Shakhova, N., I. Semiletov, A. Salyuk, V. Yusupov, D. Kosmach, and O. Gustafsson (2010b), Extensive methane venting to the atmosphere from sediments of the East Siberian Arctic Shelf, *Science*, 327, 1246–1250, doi:10.1126/science.1182221.

Shindell, D. T., et al. (2006), Multimodel simulations of carbon monoxide: Comparison with observations and projected near-future changes, *J. Geophys. Res.*, 111, D19306, doi:10.1029/2006JD007100.

Solberg, S., Ø. Hov, A. Søvde, I. S. A. Isaksen, P. Coddeville, H. De Backer, C. Forster, Y. Orsolini, and K. Uhse (2008), European surface ozone in the extreme summer 2003, *J. Geophys. Res.*, 113, D07307, doi:10.1029/2007JD009098.

Soloviev, V. A., G. D. Ginzburg, E. V. Telepnev, and Y. N. Mikhaluk (1987), *Cryothermia and gas hydrates in the Arctic Ocean*, 150 pp., Sevmorgeologia, Leningrad, Russia.

Søvde, O. A., M. Gauss, S. P. Smyshlyaev, and I. S. A. Isaksen (2008), Evaluation of the chemical transport model Oslo CTM2 with focus on Arctic winter ozone depletion, *J. Geophys. Res.*, 113, D09304, doi:10.1029/2007JD009240.

Tarnocai, C., J. G. Canadell, E. A. G. Schuur, P. Kuhry, G. Mazhitova, and S. Zimov (2009), Soil organic carbon pools in the northern circumpolar permafrost region, *Global Biogeochem. Cycles*, 23, GB2023, doi:10.1029/2008GB003327.

Walter, K. M., S. A. Zimov, J. P. Chanton, D. Verbyla, and F. S. Chapin (2006), Methane bubbling from Siberian thaw lakes as a positive feedback to climate warming, *Nature*, *443*(7107), 71–75, doi:10.1038/nature05040.

Walter, K. M., L. C. Smith, and F. S. Chapin (2007), Methane bubbling from northern lakes: Present and future contributions to the global methane budget, *Philos. Trans. R. Soc. A*, *365*(1856), 1657–1676.

Westbrook, G. K., et al. (2009), Escape of methane gas from the seabed along the West Spitsbergen continental margin, *Geophys. Res. Lett.*, *36*, L15608, doi:10.1029/2009GL039191.

Wickland, K. P., R. G. Striegl, J. C. Neff, and T. Sachs (2006), Effects of permafrost melting on CO_2 and CH_4 exchange of a poorly drained black spruce lowland, *J. Geophys. Res.*, *111*, G02011, doi:10.1029/2005JG000099.

WMO (2003), Scientific Assessment of Ozone Depletion: 2002, Global Ozone Research and Monitoring Project, report, 498 pp., Geneva.

Zimov, S. A., Y. V. Voropaev, I. P. Semiletov, S. P. Davidov, S. F. Prosiannikov, F. S. Chapin, M. C. Chapin, S. Trumbore, and S. Tyler (1997), North Siberian lakes: A methane source fueled by Pleistocene carbon, *Science*, *277*(5327), 800–802, doi:10.1126/science.277.5327.800.

M. Gauss, Norwegian Meteorological Institute, N-0313 Oslo, Norway.

I. S. A. Isaksen, Department of Geosciences, University of Oslo, N-0315 Oslo, Norway. (i.s.a.isaksen@geo.uio.no)

G. Myhre, CICERO, N-0318 Oslo, Norway.

C. Ruppel, U.S. Geological Survey, Woods Hole, MA 02543, USA.

K. M. Walter Anthony, Water and Environmental Research Center, Institute of Northern Engineering and International Arctic Research, University of Alaska, Fairbanks, AK 99775, USA.